Rerouting of ribosomal proteins into splicing in plant organelles

Chuande Wang[a], Rachel Fourdin[a], Martine Quadrado[a], Céline Dargel-Graffin[a], Dimitri Tolleter[b], David Macherel[b], and Hakim Mireau[a,1]

[a]Institut Jean-Pierre Bourgin, Institut National de Recherche pour l'Agriculture, l'Alimentation et l'Environnement (INRAE), AgroParisTech, Université Paris-Saclay, 78000, Versailles, France; and [b]Université d'Angers, Unité Mixte de Recherche 1345, Institut de Recherche en Horticulture et Semences, 49045 Angers, France

Edited by Alan M. Lambowitz, The University of Texas at Austin, Austin, TX, and approved October 1, 2020 (received for review March 6, 2020)

Production and expression of RNA requires the action of multiple RNA-binding proteins (RBPs). New RBPs are most often created by novel combinations of dedicated RNA-binding modules. However, recruiting existing genes to create new RBPs is also an important evolutionary strategy. In this report, we analyzed the eight-member uL18 ribosomal protein family in *Arabidopsis*. uL18 proteins share a short structurally conserved domain that binds the 5S ribosomal RNA (rRNA) and allows its incorporation into ribosomes. Our results indicate that *Arabidopsis* uL18-Like proteins are targeted to either mitochondria or chloroplasts. While two members of the family are found in organelle ribosomes, we show here that two uL18-type proteins function as factors necessary for the splicing of certain mitochondrial and plastid group II introns. These two proteins do not cosediment with mitochondrial or plastid ribosomes but instead associate with the introns whose splicing they promote. Our study thus reveals that the RNA-binding capacity of uL18 ribosomal proteins has been repurposed to create factors that facilitate the splicing of organellar introns.

ribosomal protein | intron splicing | plants | mitrochondria | chloroplasts

The evolution of eukaryotic cells has involved the acquisition of highly specialized energy-producing organelles such as mitochondria and plastids, both of which are of bacterial origin (1, 2). The transformation of the original endosymbionts into specialized organelles involved a massive reduction of their genomes and a progressive loss of their autonomy. A large number of host-derived factors, either acquired or recruited during evolution, became necessary for proper expression of the essential genes present in modern mitochondrial and plastid genomes. The interplay between ancient bacterial-derived processes and eukaryotic-derived functions resulted in organellar gene expression mechanisms that are more complex than those of modern bacteria (3, 4). Consequently, the production and the expression of mitochondrial and plastid transcripts is highly complex, especially in plants. Angiosperm mitochondrial and plastid genomes produce an array of monocistronic and polycistronic transcripts that undergo nucleolytic processing, extensive sequence modification through C-to-U RNA editing, and removal of multiple group II introns prior to translation. Each of these RNA processing steps requires the action of dedicated ribonucleoprotein complexes that are still poorly characterized. Several classes of nuclear-encoded RNA-binding proteins were found to play roles in mitochondrial and/or plastid RNA expression including the pentatricopeptide repeat (PPR) proteins (5, 6) and other kinds of helical repeat protein families (7), which all adopt similar solenoid-like structures exposing key amino acids for RNA binding (7–9). Other protein families like RNA recognition motif (RRM) factors, multiple organellar RNA editing factors (MORF), chloroplast RNA splicing and ribosome maturation (CRM), or plant organellar RNA recognition (PORR) families as well as maturases also play roles in plant organellar RNA expression (10–14). Some of these factors were created out of generic RNA-binding domains (such as the RRM domain) while others evolved by hijacking proteins with different functions such as the CRM proteins that are likely derived from a bacterial protein involved in ribosome maturation (11). Ribosomal proteins (RPs) represent another large class of conserved and abundant RNA-binding proteins. Although they are primarily involved in protein synthesis, extraribosomal functions have been described in a few cases (15–17). Plant RPs are often encoded by small multigene families comprising up to eight active genes, suggesting potential specialization or extraribosomal activities for some family members (18, 19). In this study, we investigated the function of a small protein family in *Arabidopsis* whose members were annotated to be homologs of the uL18 RP. The detailed analysis of two of these uL18 homologs revealed that they have lost the ability to associate with ribosomes and have become organellar group II intron splicing factors.

Results

The uL18 Protein Family Comprises Eight Members in *Arabidopsis*. While analyzing sequence variability among RPs in *Arabidopsis*, we noticed that eight proteins were classified in the L18pL5e superfamily. These proteins share a rather degenerate but structurally conserved C-terminal RNA-binding domain forming three α-helices and three and a half β-sheets that was shown to bind the 5S ribosomal RNA (rRNA) (20) (Fig. 1). C-terminal GFP translational fusions with each of these uL18-Like proteins revealed that five members are targeted to mitochondria and three to plastids (Fig. 2). Multiple sequence alignments indicated that uL18-Like members are more homologous to the *Escherichia coli* uL18 protein than to the cytosolic uL18, strongly suggesting a bacterial origin for the uL18-Like family (*SI Appendix*, Fig. S1). Moreover, two members of the uL18 family, AT1G48350 and AT5G27820, have sequences and sizes very close to the *E. coli*

Significance

Ribosomal proteins (RPs) are essential structural components of ribosomes. In many instances, RPs are encoded in small families of genes, suggesting possible neofunctionalization for some family members. This is the case of the uL18 family of proteins that developed during plant evolution and which is composed of eight members in most Angiosperms. Our study shows that two members associate with organellar ribosomes while two other uL18-Like proteins have become intron-specific splicing factors acting in mitochondria and plastids, respectively. Our study shows that the RNA binding capacity of RPs can be diverted to create factors acting in intron splicing.

Author contributions: H.M. designed research; C.W., R.F., M.Q., C.D.-G., D.T., and D.M. performed research; C.W. and H.M. analyzed data; and C.W. and H.M. wrote the paper.

The authors declare no competing interest.

This article is a PNAS Direct Submission.

[1]To whom correspondence may be addressed. Email: hakim.mireau@inrae.fr.

This article contains supporting information online at https://www.pnas.org/lookup/suppl/doi:10.1073/pnas.2004075117/-/DCSupplemental.

First published November 9, 2020.

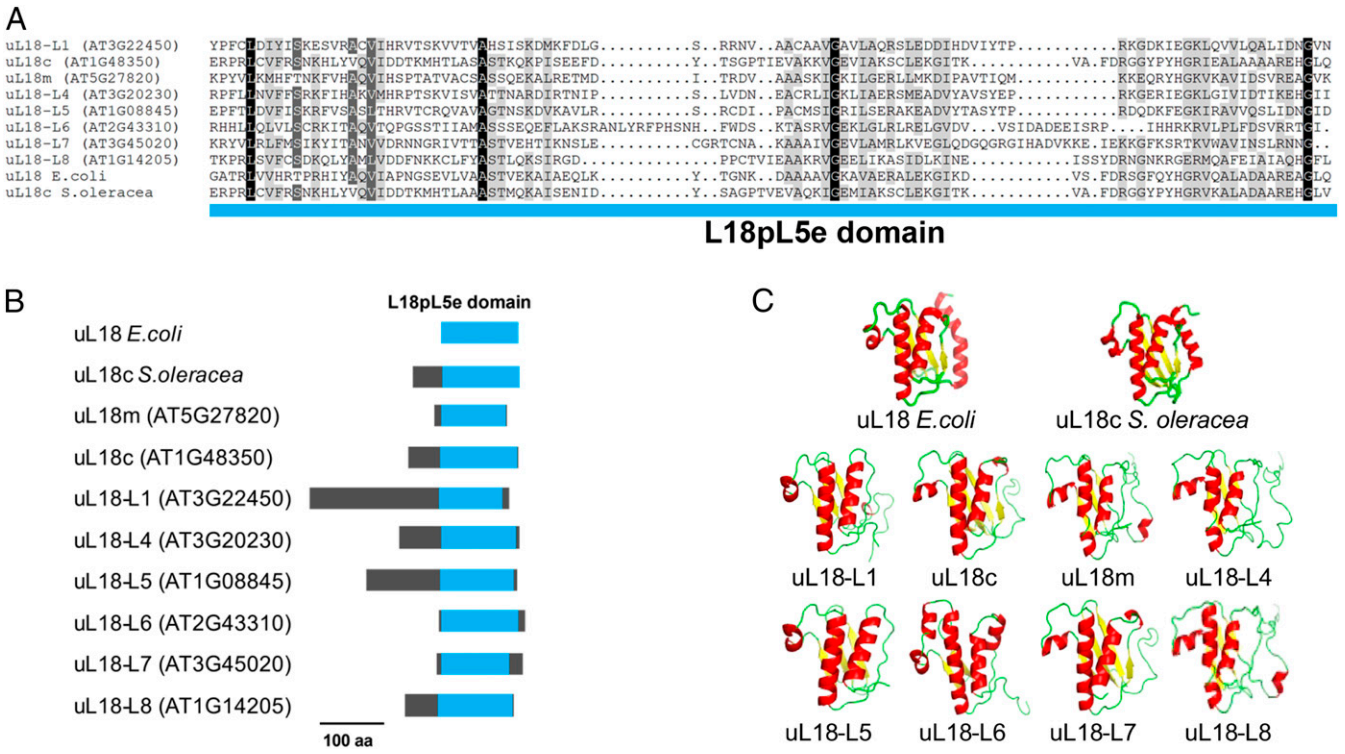

Fig. 1. The *Arabidopsis* nuclear genome encodes eight different uL18-Like proteins. (*A*) Sequence alignment of the C-terminal L18pL5e domain of the eight uL18-Like *Arabidopsis* proteins, the uL18 protein from *E. coli* and the uL18c from *S. oleracea*. The residues are colored according to the percentage of conservation from dark gray (100% identical) to light gray (50% identical). (*B*) Diagrams showing in blue the position of the L18pL5e domain in *Arabidopsis* uL18-Like, *E. coli* uL18, and *S. oleracea* uL18c proteins. (*C*) Three-dimensional structures depicting the three α-helices and three and a half β-sheets of the L18pL5e RNA binding domain as present in the *E. coli* uL18 (Protein Data Bank [PDB] ID code: 4YBB) and the *S. oleracea* plastid uL18c (PDB ID code: 5MMM) and predicted for the eight uL18-Like *Arabidopsis* proteins. β-sheets are shown in yellow and α-helices in red. The predicted structural models for the eight uL18-Like *Arabidopsis* proteins were generated with Phyre2.

uL18 protein. A protein 81% identical to the mature form of AT1G48350 was found in the structure of the spinach (*Spinacia oleracea*) chloroplast ribosome (21), indicating that it most likely corresponds to the plastid uL18 protein in *Arabidopsis*. We thus named this protein uL18c in agreement with the new RP nomenclature (22). Similarly, the AT5G27820 protein was recently found to be a component of the mitochondrial ribosome (23) and was thus termed uL18m (Fig. 1). Our GFP fusion analysis confirmed the plastid and mitochondrial targeting of *Arabidopsis* uL18c and uL18m, respectively (Fig. 2). The function of the six other proteins could not be recognized from their sequence and were named uL18-Like (or uL18-L) proteins. Potential orthologs could be easily identified for most uL18-Like members in both monocots and dicots, supporting their essential character for organelle functions (*SI Appendix*, Fig. S1). The only exception is the uL18-L6 protein, which appears to be absent in monocotyledons.

***ul18-l1* Mutant Plants Have a Strongly Retarded Growth Phenotype.** To gain insight into the function of uL18-Like proteins, we first identified a mutant in the *uL18-L1* gene (Fig. 3*A*). Under conventional greenhouse conditions, homozygous *ul18-l1* plants displayed a marked slow growth phenotype and harbored small twisted leaves (Fig. 3*B*). The mutant plants were late flowering and produced seeds with lower germination capacity compared to the wild type (Fig. 3*B*). All these phenotypes could be complemented by the expression of an HA-tagged copy of uL18-L1 in the mutant, supporting the view that the observed alterations were due to the inactivation of AT3G22450 (Fig. 3*B*). The mitochondrial localization of uL18-L1 was then confirmed by probing total, plastid, and mitochondrial protein fractions prepared from complemented plants (*SI Appendix*, Fig. S2). Collectively, the results demonstrated the strict mitochondrial localization of the uL18-L1 protein.

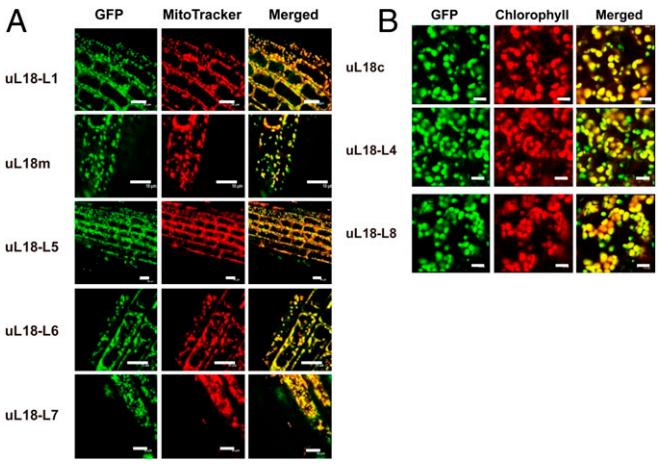

Fig. 2. The *Arabidopsis* uL18 and uL18-Like proteins are transported into mitochondria or plastids. Confocal microscope images showing the subcellular distribution of GFP translational fusions involving the indicated uL18 and uL18-Like proteins. (*A*) Pictures taken from root cells of young *Arabidopsis* transgenic plants. (*Left*) GFP fluorescence. (*Center*) Mitotracker Red marker. (*Right*) Merged signals. (*B*) Pictures taken from leaf cells of *Arabidopsis* transgenic plants. (*Left*) GFP fluorescence. (*Center*) Chlorophyll fluorescence. (*Right*) Merged signals. (Scale bars, 10 μm.)

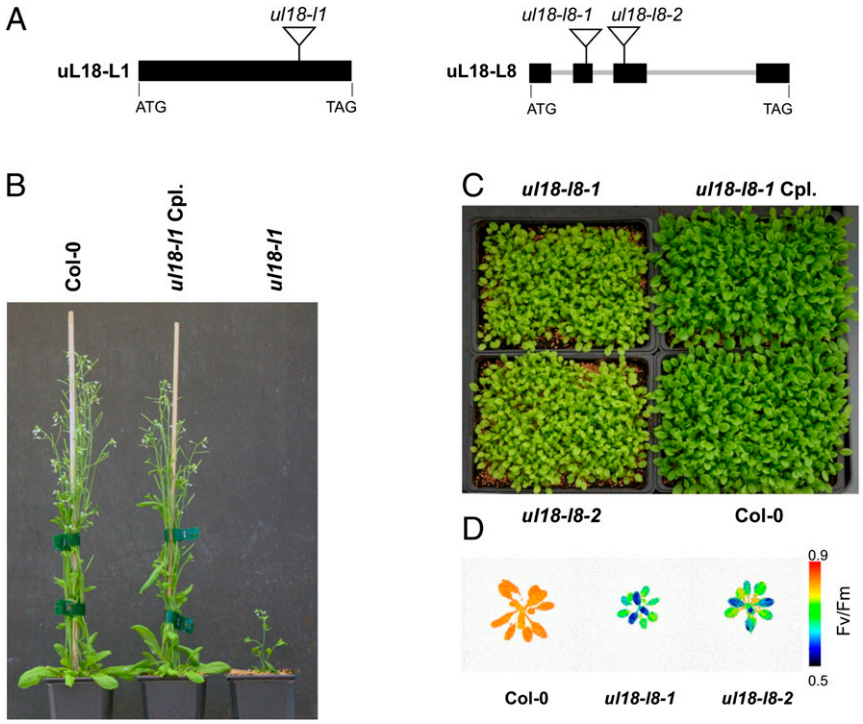

Fig. 3. *ul18-l1* and *ul18-l8* mutants display altered developmental phenotypes. (*A*) Schematic representations of *uL18-L1* and *uL18-L8* gene structures with exons shown as black boxes and introns as thick gray lines. Triangles indicate the positions of T-DNA insertions in corresponding mutant alleles. (*B*) Photograph of 8-wk-old plants showing the reduced size of *ul18-l1* homozygous mutants compared with WT and genetically complemented (Cpl) plants. (*C*) Photograph of 4-wk-old plants at the rosette stage showing the slightly reduced size and pale green color of *ul18-l8* homozygous mutants compared with WT and genetically complemented (Cpl) plants. (*D*) False-color images representing Fv/Fm ratios of 4-wk-old WT (Col-0), *ul18-l8-1*, and *ul18-l8-2* plants. The color scale indicates Fv/Fm signal intensities.

***ul18-l1* Mutant Plants Show Strongly Reduced Levels of Respiratory Complex I.** The mitochondrial localization of the uL18-L1 protein strongly suggested that the developmental alterations of *ul18-l1* plants could result from altered respiration. We thus monitored the levels of the different respiratory complexes in comparison with the wild type by blue-native gel analysis. Immunoblot analyses revealed only trace amounts of fully assembled complex I in *ul18-l1* plants and an overaccumulation of complex IV as well as a 450-kDa complex I assembly intermediate in the mutant (Fig. 4*A*). In-gel activity staining confirmed the marked reduction of respiratory complex I in *ul18-l1* plants and an overabundance of complex IV (*SI Appendix*, Fig. S3), which correlated with increased steady-state levels of Cox1, Cox2, and cytochrome *c* (Fig. 4*B*). The reduction in complex I activity in the *ul18-l1* mutant was further confirmed by in vitro root growth assays, which revealed a much weaker sensitivity of *ul18-l1* plants to rotenone compared to the wild type (*SI Appendix*, Fig. S3*B*). Although rotenone reduces root growth in both WT and mutant plants, at the highest dose the inhibition in the wild type is close to 50%, whereas it is limited to only 10% in the *ul18-l1* mutant. Further, we could detect an overexpression of several components of the alternative respiratory pathway in *ul18-l1* plants, including the alternative mitochondrial NADH dehydrogenase *NDB4* and the alternative oxidase (Fig. 4*B* and *SI Appendix*, Fig. S4). These results indicated that uL18-L1 is crucial for the biogenesis and activity of mitochondrial complex I.

The uL18-L1 Protein Is Required for the Splicing of Two Mitochondrial Introns. Because of their homology to uL18, we suggested that uL18-type proteins may be RNA-binding proteins as well and that the uL18-L1 protein could therefore play a key role in the production of one or several mitochondria-encoded RNAs. To test this hypothesis, we determined the steady-state levels of mature and precursor mitochondrial transcripts by qRT-PCR (*SI Appendix*, Fig. S5) and calculated the splicing efficiency of mitochondrial introns in both WT and *ul18-l1* plants (Fig. 4*C*). A highly pronounced decrease in the splicing efficiency of *nad5* intron 4 as well a weaker reduction for *nad2* intron 1 splicing could be detected in *ul18-l1* plants (Fig. 4*C*). A global overexpression of other premature and mature mitochondrial messenger RNAs (mRNAs) was also detected in the mutant (*SI Appendix*, Fig. S5 *A* and *B*). This response is often observed in respiratory mutants (24, 25) and likely plays a role in compensating for their decreased respiratory capacity. RNA gel blots confirmed these observations and indicated that no detectable amount of mature *nad5* mRNA could be found in the *ul18-l1* mutant (Fig. 4 *D*–*F*). The decrease in *nad2* intron 1 splicing was also verified, but the production of mature *nad2* mRNA was much less affected than that of *nad5* and is therefore less likely to limit the production of complex I in *ul18-l1* plants (Fig. 4 and *SI Appendix*, Fig. S5). Altogether, these results indicated that the uL18-L1 protein is essential for the *cis*-splicing reaction involving *nad5* intron 4 and, to a lesser extent, also for the removal of *nad2* intron 1.

The *ul18-l8* Mutant Plants Display Altered Photosynthesis. To further explore the functions of uL18-Like proteins, we isolated two transfer DNA (T-DNA) insertion mutants, *ul18-l8-1* and *ul18-l8-2*, in the *uL18-L8* gene, whose encoded protein is transported into plastids (Fig. 2*B*). Both mutant lines displayed a pale green phenotype associated with a slightly retarded growth (Fig. 3*C*). These alterations could be reversed by expression of an HA-tagged copy of uL18-L8 in one of the mutants, confirming that they were produced by the inactivation of *uL18-L8*. Pigment

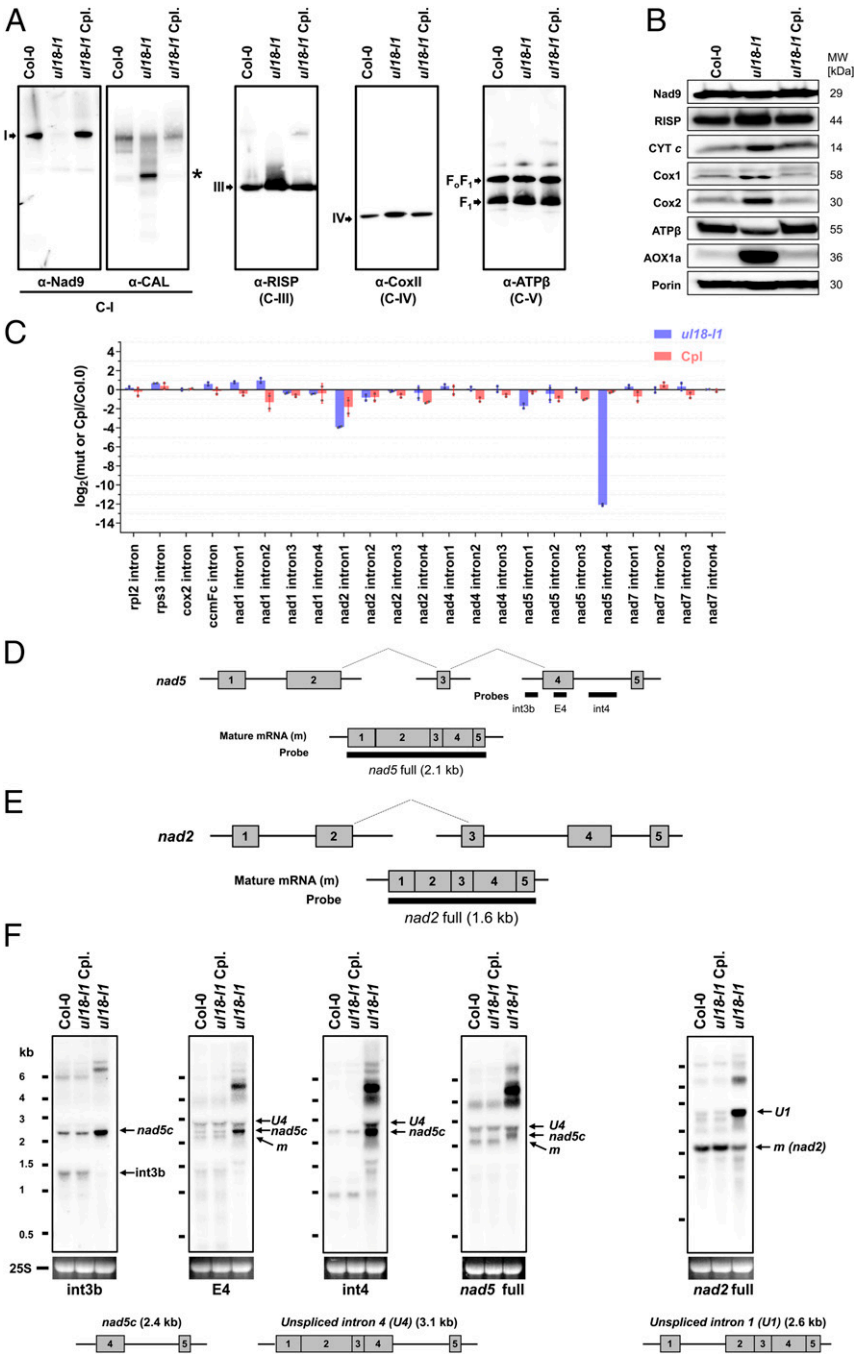

Fig. 4. *ul18-l1* plants are defective in complex I and are impaired in *nad5* intron 4 and *nad2* intron 1 splicing. (*A*) Immunodetection of respiratory complexes in blue native polyacrylamide gel electrophoresis [*PAGE*] blots made from mitochondrial extracts of WT (Col-0), *ul18-l1* mutant, and complemented (Cpl) plants. Antibodies to Nad9 and CAL proteins were used to detect fully assembled and assembly intermediates of complex I (C-I), respectively. Complex III (C-III) was detected with antibodies to the RISP protein, complex IV (C-IV) with anti-Cox2 antibodies, and complex V (C-V) with anti-ATPβ antibodies (see *SI Appendix*, Table S2 for details). Respiratory complexes are designated by Roman numerals, and the asterisk designates a complex I assembly intermediate. (*B*) SDS/PAGE immunoblots performed on total mitochondrial protein extracts prepared from the indicated genotypes (see *A* for details) and probed with antibodies to subunits of respiratory complex I (Nad9), complex III (RISP), complex IV (Cox1 and Cox2), the complex V (ATPβ), cytochrome *c* (CYT c), and the alterative oxidase (AOX). Porin was used as protein loading control. (*C*) qRT-PCR analysis measuring the splicing efficiencies of mitochondrial introns in *ul18-l1* (blue bars) and complemented (Cpl, red bars) plants. The bars depict $\log_2$ ratios of splicing efficiencies in *ul18-l1* and complemented plants to the wild type (Col-0). Three technical replicates and two independent biological repeats were used for each genotype. SD are indicated. (*D*) Schematic representation of the three *nad5* precursor transcripts, which are fused by two *trans*-splicing events to produce the mature (m) *nad5* mRNA. Gray boxes indicate exons. Introns and 5′ and 3′ UTRs are shown as thin lines. The probes used to interpret RNA gel blot results are also indicated. (*E*) Schematic representation of *nad2* precursors and mature mRNA, using the same iconography as in *D*. (*F*) RNA gel blots showing the accumulation profiles of *nad5* and *nad2* transcripts in the *ul18-l1* mutant compared to WT (Col-0) and complemented plants (Cpl). Used probes are indicated below hybridization results. Ethidium bromide staining of the 25S ribosomal RNA serves as a loading control. Schematic representations and sizes of the *nad5* transcript with unspliced intron 4 (*nad5* U4), *nad5c*, and *nad2* transcript with unspliced intron 1 (*nad2* U1) are depicted below the blots to help interpreting the results. The apparent size of *nad5* U4 is smaller than expected due to a congestion by near-sized 25S rRNA (24). RNA marker sizes are indicated (kilobases). E, exon; int, intron; m, mature mRNAs.

composition revealed that both mutants have a slight decrease in chlorophyll and carotenoid contents (*SI Appendix*, Table S4). Chlorophyll fluorescence further showed that the maximum quantum efficiency of PSII (Fv/Fm) was decreased by around 11% in both allelic mutants (*SI Appendix*, Fig. S4 and Fig. 3*D*) and that fraction of open PSII centers (qL) decreased by 40%. Moreover, immunoblots of subcellular fractions revealed that uL18-L8 is enriched in isolated chloroplasts and is detected solely in the stromal fraction (*SI Appendix*, Fig. S2). Overall, this analysis demonstrated that the loss of the uL18-L8 protein has a moderate but significant impact on the light energy efficiency of photosynthesis.

The uL18-L8 Protein Is Required for the Splicing of the First Intron of *rps12* in Plastid. To get insight into the function of uL18-L8, qRT-PCR analysis was performed to comparatively measure the steady-state level of plastid-encoded transcripts in *ul18-l8* plants. We first observed that no plastid transcript suffered from global mRNA destabilization in either of the mutants (*SI Appendix*, Fig. S6). However, an ∼64-fold decrease in the splicing efficiency of the first intron of the *rps12* transcript could be detected (Fig. 5*A*). This reduction is partially compensated by a general overaccumulation of plastid transcripts, resulting in mature *rps12* mRNA being around 13-fold less abundant in *ul18-l8* plants compared to the wild type (*SI Appendix*, Fig. S6*A*). The mature *rps12* ORF is contained in a dicistronic transcript with *rps7* and is produced via a *trans*-splicing reaction involving a first precursor comprising the first exon of *rps12* plus *rpl20* and a second precursor carrying the last two *rps12* exons as well as the *rps7* gene (Fig. 5*B*). RNA gel blot analysis showed that very low amounts of mature *rps12* dicistronic mRNA are detected in *ul18-l8* plants and that both *rps12* precursor transcripts overaccumulate compared to the wild type (Fig. 5*C*). The splicing efficiency of introns contained in plastid tRNAs was then evaluated by RNA blot analysis and did not show any reduction (*SI Appendix*, Fig. S7*A*). It however revealed that most mature plastid tRNAs overaccumulated in both mutants (*SI Appendix*, Fig. S7*A*). Further RNA blots showed normal steady-state levels for the 23S, 4.5S, and 5S rRNAs in *ul18-l8* plants (*SI Appendix*, Fig. S7*B*), whereas 16S rRNA levels show an ∼30% reduction in the mutants (Fig. 5*D* and *SI Appendix*, Fig. S7*C*). Immunoblots of leaf extracts revealed that reduced amounts of Rps12 could be detected in the *ul18-l8* mutants (Fig. 5*E*), which is coherent with the reduction of *rps12* intron splicing detected in these plants (Fig. 5*A*). Indeed, a reduction in the steady-state levels of all tested plastid-encoded proteins (Rps12, Rps1, Rps7, PsbD, PetA, PetB, and AtpF) was also observed in *ul18-l8* plants. These proteins accumulated at about 50% of WT levels, indicating that a 13-fold decrease in mature *rps12* mRNA production in *ul18-l8* mutants results in a reduction of only half of Rps12 protein level and plastid translation. Conversely, the level of the nuclearly encoded plastocyanin was found unchanged in the mutants (Fig. 5*E*).

Overall, these results demonstrated that the uL18-L8 protein is required for the *trans*-splicing reaction involving the first intron of *rps12* in plastids and that *ul18-l8* mutants consequently produce reduced levels of the Rps12 RP, resulting in a significant decrease in the production of several plastid-encoded proteins and 16S rRNA accumulation.

uL18-L1 and uL18-L8 Do Not Associate with Mitochondrial or Plastid Ribosomes. To see whether the uL18-L1 and uL18-L8 proteins conserved a capacity to associate with mitochondrial or plastid ribosomes, the sizes of complexes containing these two proteins were measured by density gradient sedimentation. Most previously identified mitochondrial or plastid group II intron splicing factors reside in high molecular mass ribonucleoprotein complexes that are, however, lighter than ribosomes (12, 26). Mitochondrial or stromal extracts prepared from *ul18-l1* and *ul18-l8-1* complemented plants were fractionated on sucrose gradient and the recovered fractions were analyzed by immunoblot assays. Both uL18-Like proteins were found in particles that were much smaller than mitoribosomes or chlororibosomes (Fig. 6). Interestingly, uL18-L8 was found in lighter fractions compared with the plastid splicing factor mTERF4 (27). Identical results were obtained with overexpressing *Arabidopsis* cell lines in which the detection of uL18-L1 and uL18-L8 is greatly facilitated compared to organelles purified from complemented plants (*SI Appendix*, Fig. S8*A*). Both proteins could be immunoprecipitated from these transgenic lines but none of the tested anti-ribosome antibodies indicated coenrichment with mitoribosomes for uL18-L1 or chlororibosomes for uL18-L8 (*SI Appendix*, Fig. S8*B*).

uL18-L1 and uL18-L8 Associate In Vivo with Introns Whose Splicing They Facilitate. To identify intron RNAs that associate with uL18-L1 and uL18-L8 in vivo, both proteins were immunoprecipitated from overexpressing *Arabidopsis* cell lines with HA antibody and coenriched RNAs were purified from the coimmunoprecipitates. Obtained RNAs were then used for cDNA synthesis and analyzed by qPCR using primer pairs amplifying mitochondrial or plastid precursor mRNAs. Enrichment ratios were calculated in comparison to control immunoprecipitations performed with IgG-Protein A magnetic beads. We observed a very high and specific enrichment of uL18-L1 with *nad5* intron 4 and uL18-L8 with *rps12* intron 1 (Fig. 7). Interestingly, *nad2* intron 1 was not coenriched in uL18-L1 immunoprecipitates, suggesting that *nad2* intron 1 splicing defect detected in *ul18-l1* plants could be a secondary effect of complex I deficiency as observed in several independent *Arabidopsis* complex I mutants (28–32). Both uL18-type proteins thus associate with their genetic target in vivo, supporting a direct role in the splicing of the concerned introns.

Discussion

The uL18 RNA Binding Domain Was Recruited Early in the Evolution of Terrestrial Plants to Produce Intron-Specific Splicing Factors for Organelles. RPs are essential components of ribosomes that help structuring rRNAs to allow them to function optimally in protein synthesis. In recent years, several lines of evidence have documented that RPs can carry ribosome-independent functions (15, 33, 34). In this report, we reveal that two *Arabidopsis* proteins of the uL18 family play essential roles in group II intron splicing in chloroplasts or mitochondria. The uL18-L1 protein was found to be required for the splicing of last intron contained in *nad5* pre-mRNAs in mitochondria, whereas the plastid uL18-L8 is required for the removal of *rps12* intron 1 (Fig. 8). In both mutants, the observed splicing reductions are associated with an overaccumulation of various splicing intermediates whose analysis will be instructive to better understand the mechanism and orchestration of splicing of group II introns in organelles. Moreover, these two factors are not similarly required for the splicing reactions they promote. The loss of uL18-L1 results in a very strong reduction in *nad5* intron 4 splicing while the decrease in *rps12* intron 1 splicing in *ul18-l8* plants is much less pronounced and leads to moderate pale-green photosynthetic mutants. Other nuclear-encoded transfactors such as PPR4 or EMB2654 have proven to be more critical for *rps12* intron 1 splicing, and their loss leads to embryo lethality in *Arabidopsis* and seedling-lethal plants in maize, highlighting the essentiality of Rps12 and plastid translation for plant survival (35–38). *Arabidopsis* knockdown mutants for these two genes result in severely discolored plants that are not always associated with a greater decrease in *rps12* intron 1 splicing compared to *ul18-l8* mutants (36–38). However, side-by-side comparisons to notably measure residual Rps12 protein in these different mutants

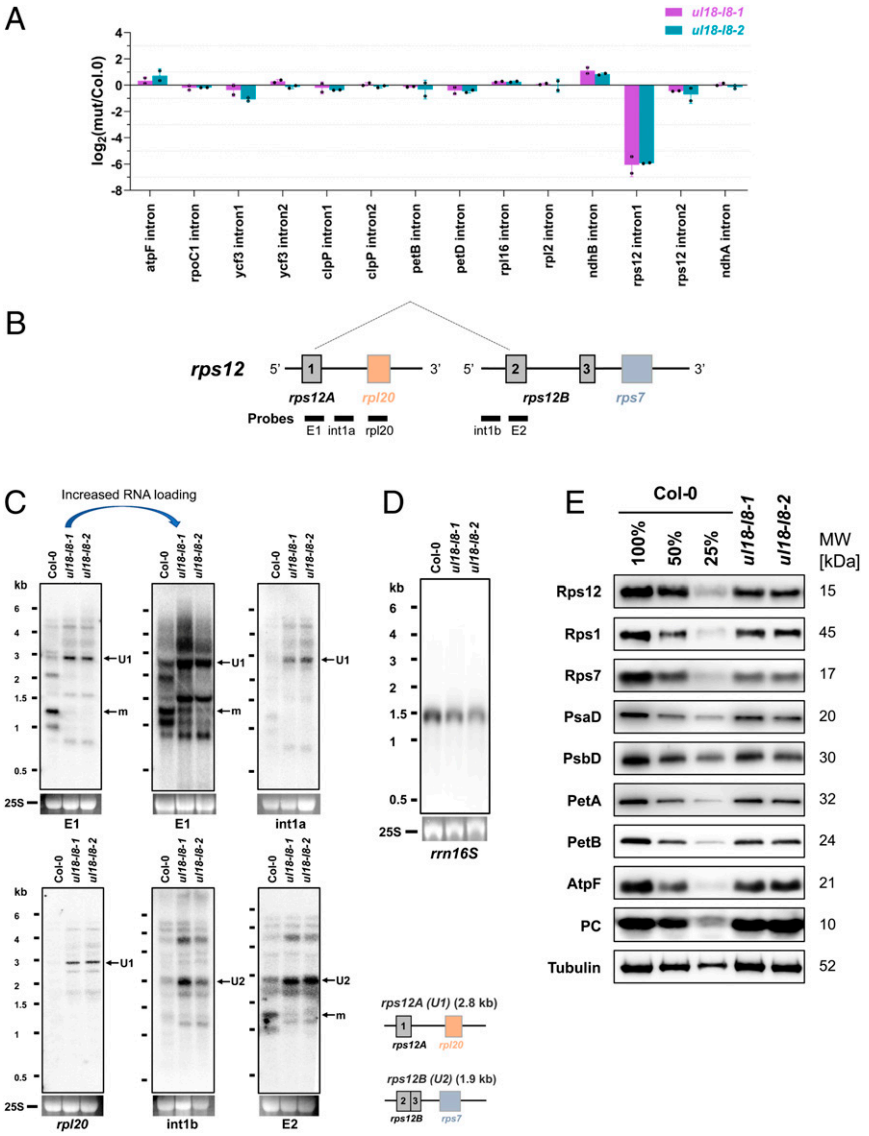

Fig. 5. The *ul18-l8* mutants have reduced levels of *rps12* intron 1 splicing and underaccumulate plastid-encoded proteins. (*A*) qRT-PCR analysis measuring the splicing efficiencies of plastid introns in *ul18-l8* mutants. The bars show $\log_2$ ratios of splicing efficiencies in *ul18-l8* plants to the wild type (Col-0). Three technical replicates and two independent biological repeats were used for each genotype; SDs are indicated. (*B*) Schematic representation of the two *rps12* precursor transcripts that are fused by *trans*-splicing to produce the mature (m) *rps12* mRNA. Gray and colored boxes indicate exons. Introns and 5′ and 3′ UTRs are shown as thin lines. The probes used to interpret RNA gel blot results are shown. (*C*) RNA gel blot analyses showing the accumulation patterns of *rps12* transcripts in *ul18-l8* mutants in comparison with the wild type. Used probes are specified below each blot. A second blot with increased RNA loading (15 μg) was done for the *rps12* E1 probe to better visualize the low amounts of mature *rps12* transcript that accumulate in *ul18-l8* mutants. Ethidium bromide staining of the 25S ribosomal RNA serves as a loading control. Schematic representations and sizes of unspliced *rps12A* (U1) and *rps12B* (U2) precursor transcripts are depicted below the blots. RNA marker sizes are indicated (kilobases). E, exon; int, intron; m, mature mRNA. (*D*) RNA gel blot showing the abundance of the 16S rRNA in the wild type (Col-0) and in *ul18-l8* mutants. (*E*) Immunodetection of photosynthetic chain proteins on SDS/PAGE blots in *ul18-l8* mutants compared to the wild type. Total proteins purified from the indicated genotypes were probed with antibodies to subunits of the chloroplast ATP synthase (AtpF), photosystem II (PsbD), photosystem I (PsaD), the cytochrome b_6f complex (PetA and PetB), RPs (Rps12, RPS1, and Rps7) and the plastocyanin. Tubulin was used as protein loading control. Dilution series of proteins extracted from wild type (Col-0) were used for signal comparison. Protein molecular masses (MW) of detected proteins are indicated on the right.

appears indispensable to explain their phenotypic differences. The uL18-L1 protein is found in ribonucleoprotein complexes (RNPs) whose sizes are close to those corresponding to splicing factors such as the nMAT2 protein (Fig. 6 and *SI Appendix*, Fig. S8). Conversely, the uL18-L8 protein was detected in smaller RNP complexes compared to the general plastid splicing factor mTERF4. Further analyses determining the composition of these different plastid splicing complexes need to be performed to determine the origin of this size difference. The functions for these two uL18-Like factors cannot be considered as extraribosomal functions *sensu stricto*, since both uL18-L1 and uL18-L8 proteins were not found to reside in mitochondrial or plastid ribosomes, respectively (Fig. 6). Our results nevertheless support the capacity of RP binding domains to accommodate new RNA targets, and reveal that this class of proteins can acquire functions in intron splicing. These observations add support to an important evolutionary paradigm in which existing genes are duplicated and become diversified to support new functions. In the present cases, duplicated and subsequently divergent copies of *uL18m* or *uL18c* were likely selected to play roles in organellar intron splicing at some

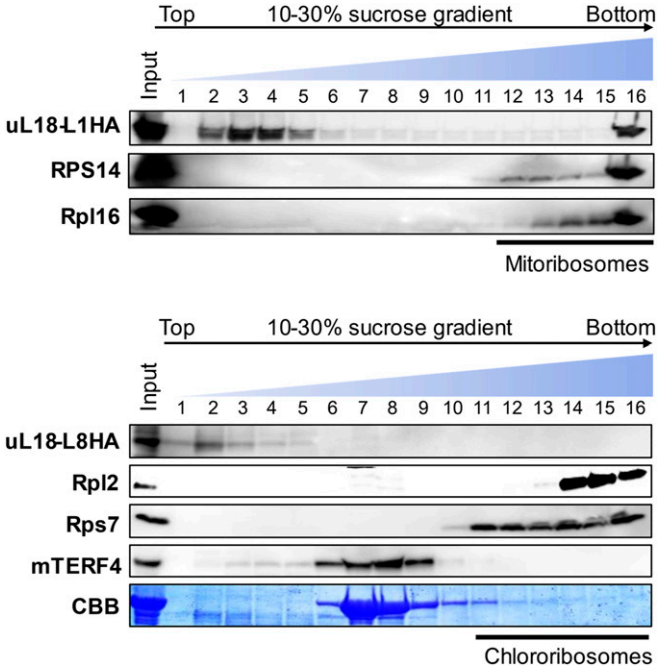

Fig. 6. uL18-L1 and uL18-L8 are not components of ribosomes. Mitochondrial (*Upper*) and stromal (*Lower*) extracts fractionated on sucrose gradients. An equal volume of each recovered fraction was analyzed by protein gel blot with the indicated antibodies. Mitochondrial Rpl16 and RPS14 as well as plastid Rpl2 and Rps7 were used to localize mitochondrial or plastid ribosomes along the gradients. mTERF4 is a protein required for the splicing of multiple plastid group II introns (27). The αHA antibody detects uL18-L1-3HA and uL18-L8-3HA fusion proteins. Coomassie brilliant blue (CBB) staining of the membrane detecting the position of the large Rubisco subunit (RbcL) in the gradient is shown below the hybridization results.

point in the evolution of plants. The search for uL18 homologs from bacteria to seed plants indicates that the diversification of the uL18 family occurred early in land plant evolution. In bacteria or algae, a single *uL18* gene can be generally recognized, which encodes a protein sharing strong homologies with the RP uL18c (*SI Appendix*, Fig. S1). Nonvascular plants encode a few more uL18-Like proteins whose closest homologs correspond to the uL18m, uL18c, and uL18-L4 proteins. Gymnosperms and angiosperms encode similar corteges of uL18 and uL18-Like proteins as in *Arabidopsis*, with the intriguing exception of uL18-L6 that is specific to dicotyledonous plants (*SI Appendix*, Fig. S1). It thus appears that the expansion of the uL18 family was initiated in nonvascular basal plants and that the first diverging uL18 member may have been the *uL18-L4* gene. These observations nicely corroborate previous analyses indicating that divergence of organellar introns from the classic structure of group II introns has occurred early in the evolution of terrestrial plants (39–41).

Organellar introns derive from bacterial counterparts and can be classified as group I or group II based on specific structural characteristics. Introns contained in vascular plants organellar genomes are mostly of type II and fold into a conserved structure comprising six helical domains (DI–DVI) that radiate from a central hub (42). Autonomous group II introns encode a maturase that is essential for intron mobility and splicing. Most organellar introns in seed plants show, however, degenerate structures compared to canonical group II introns or lack structural features that are important for removal (40, 41). Unlike in bacteria, these deviant group II introns are maintained in plant organellar genomes as splicing-only elements. They may be mobilized via unusual splicing mechanisms, but a tolerance to structural changes permitted by the selection of a compensatory accessory machinery is an evolutionary strategy that is chosen to maintain efficient splicing of derivatized introns in organelles (41, 43). Various kinds of RNA-binding proteins have been recruited to play roles in organellar intron splicing like aminoacyl tRNA synthetases, a peptidyl-tRNA hydrolase, pseudouridine synthase homologs, or proteins derived from a bacterial ribosome assembly factors (11, 44–47). Minor evolutionary tinkering thus seems sufficient to confer novel activities in intron splicing to these RNA-binding proteins, as for the uL18 homologs. By associating with their target intron, these factors could form ribonucleoprotein complexes that help intron folding and stabilize their structure in a catalytically active form (48). Advanced biochemical and structural analyses are however necessary to understand how uL18-Like proteins along with other proteinaceous factors facilitate group II intron splicing in plant organelles. Effectively, the coaction of several splicing factors is generally required for intron splicing in plant organelles. In the case of *nad5* intron 4, three nuclear-encoded PPR proteins

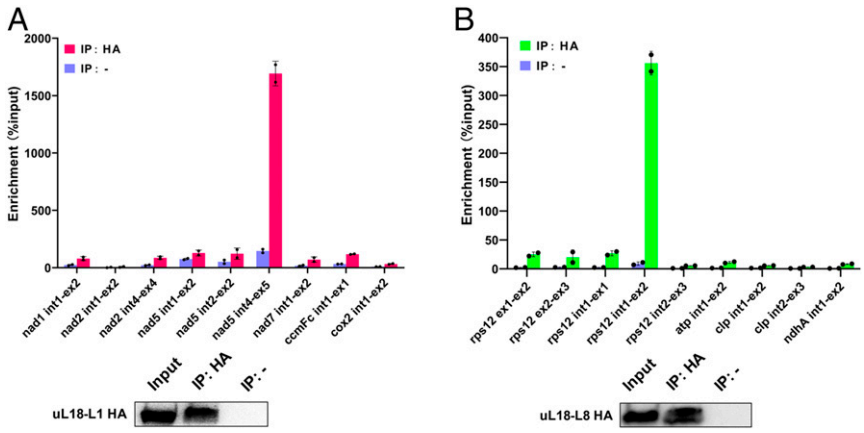

Fig. 7. uL18-L1 and uL18-L8 specifically associate with *nad5* intron 4 and *rps12* intron 1, respectively. (*A*) Analysis of RNAs that coimmunoprecipitate with uL18-L1-3HA. Total extracts from transgenic *Arabidopsis* cell lines expressing uL18-L1-3HA were used for immunoprecipitation with anti-HA antibody (IP+) and IgG-Protein A magnetic beads (IP–) as negative control. Coimmunoprecipitated RNAs were analyzed by qRT-PCR using primer pairs positioned across intron/exon junctions of the indicated mitochondrial transcripts. Enrichment ratios calculated with the delta Ct method are shown. (*B*) qRT-PCR analysis of RNAs coimmunoprecipitating with uL18-L8-3HA. Similar experiment as in *A* except that cells expressing uL18-L8-3HA were used and that primers pairs amplifying plastid transcript precursors were employed to analyze coimmunoprecipitated RNAs. Immunoblot results of input and immunoprecipitated fractions using the HA antibody (IP+) or IgG-Protein A magnetic beads (IP–) are shown.

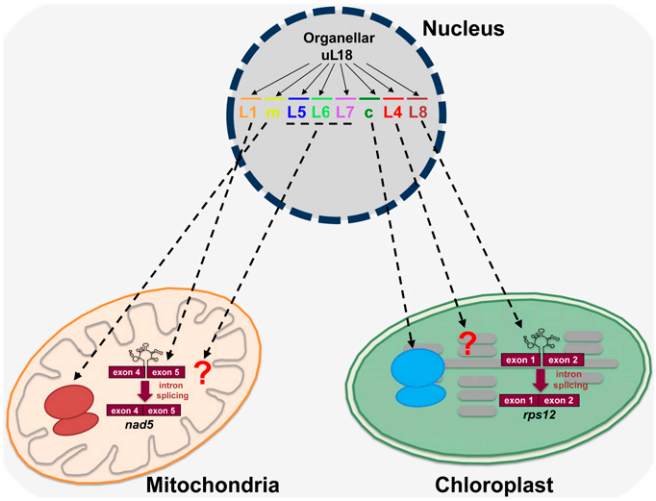

Fig. 8. Graphical summary depicting the functional diversification of the uL18 RP family in Angiosperms. The uL18 protein family comprises eight members that evolved from ancestral organellar *uL18* genes. Five members are transported into mitochondria and three into plastids. Two uL18 proteins (uL18m and very likely uL18c) have retained the original uL18 function and are subunits of organellar ribosomes. Among the other six uL18-Like members, uL18-L1 and uL18-L8 have evolved toward splicing and specifically associate in vivo with introns whose splicing they promote.

[MISF68 (24), ZmSMK9 (49), and ZmSMR1 (50)] in addition to uL18-L1 are required for its removal from pre-mRNAs. Similarly, in addition to uL18-L8, splicing factors from various protein families, namely the PPR protein PPR4 and EMB2654 (35–38), the CRM protein CAF2 (51), the PTH protein CRS2 (47), and the DEAD box helicases protein RH3 (52) also participate in *rps12* intron 1 splicing. It remains to be clarified how these factors collaborate or whether they act independently from each other in intron splicing.

The uL18-L1 and uL18-L8 Proteins Could Associate with 5S rRNA-like Structures in Their Target Intron. In most cases, the evolutionary recruitment of RPs toward new sites is permitted because the structure of newly targeted mRNA regions resembles that of rRNA domains to which they associate in the ribosomes (53–60). The uL18 protein is the most important factor for incorporating the 5S rRNA into the 50S ribosomal subunit. The 5S rRNA is a small RNA of around 120 nucleotides and adopts a conserved tertiary structure comprising various helices as well as terminal and internal loops (61). The most important structural determinants for uL18 anchoring are contained in its β domain comprising two helices plus one internal and a terminal loop (20). Upon binding, the uL18 protein increases the stability of 5S rRNA, modifies its structure, and enhances its affinity of uL5 (62, 63). Our structural predictions showed that C-terminal regions of uL18-L1 and uL18-L8 adopt the same structure as ribosomal uL18s and that the three β-sheets forming the RNA binding surface of uL18 are also found in the predicted structures of these two uL18-Like proteins (Fig. 1). This strongly suggests that the recruitment of uL18-Like proteins in splicing was permitted because regions within *nad5* intron 4 and *rps12* intron 1 likely resemble the β domain of 5S rRNA, at least enough so that uL18-L1 and uL18-L8 proteins could associate with them in a productive way. Interestingly, the recent structures of mammalian mitoribosomes showed that the uL18-binding domain can accommodate different but structurally similar RNA targets since tRNAs serve as architectural replacements for the 5S rRNA in these ribosomes (64, 65). Therefore, the search for regions within *nad5* intron 4 and *rps12* intron 1 that form secondary structures similar to the β domain of 5S rRNA may reveal the binding sites of uL18-L1 and uL18-L8. As uL18 does with 5S rRNA, the binding of uL18-L1 and uL18-L8 could induce local structural changes to the RNA regions to which they bind and, thereby, help their target intron to fold in an active form. These structural modifications may also permit the recruitment of other protein factor(s) necessary for splicing, similarly to the impact that the bacterial uL18 has on increasing the uL5-binding affinity for 5S rRNA. Finding the exact binding sites of uL18-L1 and uL18-L8 within their target introns represents an important challenge to better understand the role of uL18-L1 and uL18-L8 in group II intron splicing. Deciphering the functions of other uL18-Like proteins will reveal whether they also play roles in organellar intron splicing or whether they are involved in other RNA expression steps in plant organelles. The case of the uL18 family is an as-yet undescribed example in which a set of six independent members still cohabit with the original factors (uL18c and uL18m) from which they are derived. This provides a unique opportunity to understand the functional transitions that led the uL18 ribosomal-Like proteins to acquire roles in organellar intron splicing and maybe other RNA expression processes. Together, these results will better document how RPs can evolve toward new functions in RNA metabolism and how they can adapt to associate and process new RNA targets.

Materials and Methods

Plant materials, preparation of organelles, immunodetection of proteins, subcellular distributions, RNA analysis, RNA immunoprecipitation assays, blue native gel, sucrose density gradient centrifugation, transformation of *Arabidopsis* cell suspension cultures, and analysis of photosynthesis and pigment composition are described in *SI Appendix, Materials and Methods*.

Data Availability. All study data are included in the article and *SI Appendix*.

ACKNOWLEDGMENTS. This work was supported by Agence Nationale de la Recherche (ANR) MITRA Grant ANR-16-CE11-0024-01 (to H.M.) and the China Scholarship Council (to C.W.). The Institut Jean-Pierre Bourgin's (IJPB's) benefits from the support of Saclay Plant Sciences Grant ANR-17-EUR-0007. This work has benefited from the support of IJPB's Plant Observatory technological platforms. We thank Professor Gregory Brown (McGill University) for critical reading of the manuscript.

1. J. Martijn, J. Vosseberg, L. Guy, P. Offre, T. J. G. Ettema, Deep mitochondrial origin outside the sampled alphaproteobacteria. *Nature* **557**, 101–105 (2018).
2. S. B. Gould, R. F. Waller, G. I. McFadden, Plastid evolution. *Annu. Rev. Plant Biol.* **59**, 491–517 (2008).
3. A. Barkan, Expression of plastid genes: Organelle-specific elaborations on a prokaryotic scaffold. *Plant Physiol.* **155**, 1520–1532 (2011).
4. K. Hammani, P. Giegé, RNA metabolism in plant mitochondria. *Trends Plant Sci.* **19**, 380–389 (2014).
5. I. D. Small, N. Peeters, The PPR motif–A TPR-related motif prevalent in plant organellar proteins. *Trends Biochem. Sci.* **25**, 46–47 (2000).
6. C. Lurin *et al.*, Genome-wide analysis of Arabidopsis pentatricopeptide repeat proteins reveals their essential role in organelle biogenesis. *Plant Cell* **16**, 2089–2103 (2004).
7. K. Hammani *et al.*, Helical repeats modular proteins are major players for organelle gene expression. *Biochimie* **100**, 141–150 (2014).
8. P. Yin *et al.*, Structural basis for the modular recognition of single-stranded RNA by PPR proteins. *Nature* **504**, 168–171 (2013).
9. C. Shen *et al.*, Structural basis for specific single-stranded RNA recognition by designer pentatricopeptide repeat proteins. *Nat. Commun.* **7**, 11285 (2016).
10. H. Ruwe, C. Kupsch, M. Teubner, C. Schmitz-Linneweber, The RNA-recognition motif in chloroplasts. *J. Plant Physiol.* **168**, 1361–1371 (2011).
11. A. Barkan *et al.*, The CRM domain: An RNA binding module derived from an ancient ribosome-associated protein. *RNA* **13**, 55–64 (2007).
12. T. S. Kroeger, K. P. Watkins, G. Friso, K. J. van Wijk, A. Barkan, A plant-specific RNA-binding domain revealed through analysis of chloroplast group II intron splicing. *Proc. Natl. Acad. Sci. U.S.A.* **106**, 4537–4542 (2009).
13. C. C. Francs-Small *et al.*, A PORR domain protein required for *rpl2* and *ccmF(C)* intron splicing and for the biogenesis of c-type cytochromes in Arabidopsis mitochondria. *Plant J.* **69**, 996–1005 (2012).

14. C. Schmitz-Linneweber, M. K. Lampe, L. D. Sultan, O. Ostersetzer-Biran, Organellar maturases: A window into the evolution of the spliceosome. *Biochim. Biophys. Acta* **1847**, 798–808 (2015).
15. J. R. Warner, K. B. McIntosh, How common are extraribosomal functions of ribosomal proteins? *Mol. Cell* **34**, 3–11 (2009).
16. L. V. Aseev, I. V. Boni, [Extraribosomal functions of bacterial ribosomal proteins]. *Mol. Biol. (Mosk.)* **45**, 805–816 (2011).
17. H. Lu, Y. F. Zhu, J. Xiong, R. Wang, Z. Jia, Potential extra-ribosomal functions of ribosomal proteins in Saccharomyces cerevisiae. *Microbiol. Res.* **177**, 28–33 (2015).
18. R. P. Savada, P. C. Bonham-Smith, Differential transcript accumulation and subcellular localization of Arabidopsis ribosomal proteins. *Plant Sci.* **223**, 134–145 (2014).
19. L. Bonen, S. Calixte, Comparative analysis of bacterial-origin genes for plant mitochondrial ribosomal proteins. *Mol. Biol. Evol.* **23**, 701–712 (2006).
20. J. B. Scripture, P. W. Huber, Analysis of the binding of Xenopus ribosomal protein L5 to oocyte 5 S rRNA. The major determinants of recognition are located in helix III-loop C. *J. Biol. Chem.* **270**, 27358–27365 (1995).
21. P. Bieri, M. Leibundgut, M. Saurer, D. Boehringer, N. Ban, The complete structure of the chloroplast 70S ribosome in complex with translation factor pY. *EMBO J.* **36**, 475–486 (2017).
22. N. Ban *et al*., A new system for naming ribosomal proteins. *Curr. Opin. Struct. Biol.* **24**, 165–169 (2014).
23. F. Waltz *et al*., Small is big in Arabidopsis mitochondrial ribosome. *Nat. Plants* **5**, 106–117 (2019).
24. C. Wang, F. Aubé, M. Quadrado, C. Dargel-Graffin, H. Mireau, Three new pentatricopeptide repeat proteins facilitate the splicing of mitochondrial transcripts and complex I biogenesis in Arabidopsis. *J. Exp. Bot.* **69**, 5131–5140 (2018).
25. C. Wang *et al*., The pentatricopeptide repeat protein MTSF2 stabilizes a nad1 precursor transcript and defines the 3′ end of its 5′-half intron. *Nucleic Acids Res.* **45**, 6119–6134 (2017).
26. I. Keren *et al*., AtnMat2, a nuclear-encoded maturase required for splicing of group-II introns in Arabidopsis mitochondria. *RNA* **15**, 2299–2311 (2009).
27. K. Hammani, A. Barkan, An mTERF domain protein functions in group II intron splicing in maize chloroplasts. *Nucleic Acids Res.* **42**, 5033–5042 (2014).
28. A. F. de Longevialle *et al*., The pentatricopeptide repeat gene OTP43 is required for trans-splicing of the mitochondrial *nad1* Intron 1 in *Arabidopsis thaliana*. *Plant Cell* **19**, 3256–3265 (2007).
29. A. Koprivova *et al*., Identification of a pentatricopeptide repeat protein implicated in splicing of intron 1 of mitochondrial *nad7* transcripts. *J. Biol. Chem.* **285**, 32192–32199 (2010).
30. N. Haïli *et al*., The MTL1 pentatricopeptide repeat protein is required for both translation and splicing of the mitochondrial NADH DEHYDROGENASE SUBUNIT7 mRNA in Arabidopsis. *Plant Physiol.* **170**, 354–366 (2016).
31. N. Haïli *et al*., The pentatricopeptide repeat MTSF1 protein stabilizes the nad4 mRNA in Arabidopsis mitochondria. *Nucleic Acids Res.* **41**, 6650–6663 (2013).
32. C. Colas des Francs-Small *et al*., The pentatricopeptide repeat proteins TANG2 and ORGANELLE TRANSCRIPT PROCESSING439 are involved in the splicing of the multipartite *nad5* transcript encoding a subunit of mitochondrial complex I. *Plant Physiol.* **165**, 1409–1416 (2014).
33. R. B. Bhavsar, L. N. Makley, P. A. Tsonis, The other lives of ribosomal proteins. *Hum. Genomics* **4**, 327–344 (2010).
34. X. Zhou, W.-J. Liao, J.-M. Liao, P. Liao, H. Lu, Ribosomal proteins: Functions beyond the ribosome. *J. Mol. Cell Biol.* **7**, 92–104 (2015).
35. C. Schmitz-Linneweber *et al*., A pentatricopeptide repeat protein facilitates the trans-splicing of the maize chloroplast rps12 pre-mRNA. *Plant Cell* **18**, 2650–2663 (2006).
36. N. Aryamanesh *et al*., The pentatricopeptide repeat protein EMB2654 is essential for trans-splicing of a chloroplast small ribosomal subunit transcript. *Plant Physiol.* **173**, 1164–1176 (2017).
37. L. Tadini *et al*., Trans-splicing of plastid *rps12* transcripts, mediated by AtPPR4, is essential for embryo patterning in Arabidopsis thaliana. *Planta* **248**, 257–265 (2018).
38. K. Lee *et al*., The coordinated action of PPR4 and EMB2654 on each intron half mediates trans-splicing of *rps12* transcripts in plant chloroplasts. *Plant J.* **100**, 1193–1207 (2019).
39. O. Malek, V. Knoop, Trans-splicing group II introns in plant mitochondria: The complete set of cis-arranged homologs in ferns, fern allies, and a hornwort. *RNA* **4**, 1599–1609 (1998).
40. V. Knoop, The mitochondrial DNA of land plants: Peculiarities in phylogenetic perspective. *Curr. Genet.* **46**, 123–139 (2004).
41. L. Bonen, "Evolution of mitochondrial introns in plants and photosynthetic microbes" in *Advances in Botanical Research*, L. Maréchal-Drouard, Ed. (Elsevier, Amsterdam, 2012), pp. 155–186.
42. L. Bonen, *Cis*- and *trans*-splicing of group II introns in plant mitochondria. *Mitochondrion* **8**, 26–34 (2008).
43. U. G. Maier *et al*., Complex chloroplast RNA metabolism: Just debugging the genetic programme? *BMC Biol.* **6**, 36 (2008).
44. R. A. Akins, A. M. Lambowitz, A protein required for splicing group I introns in Neurospora mitochondria is mitochondrial tyrosyl-tRNA synthetase or a derivative thereof. *Cell* **50**, 331–345 (1987).
45. C. J. Herbert, M. Labouesse, G. Dujardin, P. P. Slonimski, The NAM2 proteins from S. cerevisiae and S. douglasii are mitochondrial leucyl-tRNA synthetases, and are involved in mRNA splicing. *EMBO J.* **7**, 473–483 (1988).
46. K. Perron, M. Goldschmidt-Clermont, J. D. Rochaix, A factor related to pseudouridine synthases is required for chloroplast group II intron trans-splicing in Chlamydomonas reinhardtii. *EMBO J.* **18**, 6481–6490 (1999).
47. B. D. Jenkins, A. Barkan, Recruitment of a peptidyl-tRNA hydrolase as a facilitator of group II intron splicing in chloroplasts. *EMBO J.* **20**, 872–879 (2001).
48. O. Fedorova, A. Solem, A. M. Pyle, Protein-facilitated folding of group II intron ribozymes. *J. Mol. Biol.* **397**, 799–813 (2010).
49. Z. Pan *et al*., ZmSMK9, a pentatricopeptide repeat protein, is involved in the cis-splicing of *nad5*, kernel development and plant architecture in maize. *Plant Sci.* **288**, 110205 (2019).
50. Z. Chen *et al*., PPR-SMR1 is required for the splicing of multiple mitochondrial introns, interacts with Zm-mCSF1, and is essential for seed development in maize. *J. Exp. Bot.* **70**, 5245–5258 (2019).
51. G. J. Ostheimer *et al*., Group II intron splicing factors derived by diversification of an ancient RNA-binding domain. *EMBO J.* **22**, 3919–3929 (2003).
52. Y. Asakura, E. Galarneau, K. P. Watkins, A. Barkan, K. J. van Wijk, Chloroplast RH3 DEAD box RNA helicases in maize and Arabidopsis function in splicing of specific group II introns and affect chloroplast ribosome biogenesis. *Plant Physiol.* **159**, 961–974 (2012).
53. M. Guillier *et al*., Translational feedback regulation of the gene for L35 in Escherichia coli requires binding of ribosomal protein L20 to two sites in its leader mRNA: A possible case of ribosomal RNA-messenger RNA molecular mimicry. *RNA* **8**, 878–889 (2002).
54. A. Serganov, A. Polonskaia, B. Ehresmann, C. Ehresmann, D. J. Patel, Ribosomal protein S15 represses its own translation via adaptation of an rRNA-like fold within its mRNA. *EMBO J.* **22**, 1898–1908 (2003).
55. U. Stelzl *et al*., RNA-structural mimicry in Escherichia coli ribosomal protein L4-dependent regulation of the S10 operon. *J. Biol. Chem.* **278**, 28237–28245 (2003).
56. H. J. Merianos, J. Wang, P. B. Moore, The structure of a ribosomal protein S8/spc operon mRNA complex. *RNA* **10**, 954–964 (2004).
57. L. G. Scott, J. R. Williamson, The binding interface between Bacillus stearothermophilus ribosomal protein S15 and its 5′-translational operator mRNA. *J. Mol. Biol.* **351**, 280–290 (2005).
58. N. Nevskaya *et al*., Ribosomal protein L1 recognizes the same specific structural motif in its target sites on the autoregulatory mRNA and 23S rRNA. *Nucleic Acids Res.* **33**, 478–485 (2005).
59. N. Choonee, S. Even, L. Zig, H. Putzer, Ribosomal protein L20 controls expression of the Bacillus subtilis infC operon via a transcription attenuation mechanism. *Nucleic Acids Res.* **35**, 1578–1588 (2007).
60. J. R. Iben, D. E. Draper, Specific interactions of the L10(L12)4 ribosomal protein complex with mRNA, rRNA, and L11. *Biochemistry* **47**, 2721–2731 (2008).
61. N. Delihas, J. Andersen, Generalized structures of the 5S ribosomal RNAs. *Nucleic Acids Res.* **10**, 7323–7344 (1982).
62. D. G. Bear, T. Schleich, H. F. Noller, R. A. Garrett, Alteration of 5S RNA conformation by ribosomal proteins L18 and L25. *Nucleic Acids Res.* **4**, 2511–2526 (1977).
63. N. Ban, P. Nissen, J. Hansen, P. B. Moore, T. A. Steitz, The complete atomic structure of the large ribosomal subunit at 2.4 A resolution. *Science* **289**, 905–920 (2000).
64. A. Brown *et al*., Structure of the large ribosomal subunit from human mitochondria. *Science* **346**, 718–722 (2014).
65. B. J. Greber *et al*., The complete structure of the large subunit of the mammalian mitochondrial ribosome. *Nature* **515**, 283–286 (2014).